



3D Finite Element Model for Recycled Asphalt Mixtures with High Percentages of Reclaimed Asphalt Pavement Rutting Simulation

M. M. Majidi Shad^a, M. M. Khabiri^{a*}, M. Arabani^b, H. Bahmani^a

^a Department of Civil Engineering, Yazd University, Yazd, Iran

^b Department of Civil Engineering, University of Guilan, Guilan, Iran

PAPER INFO

Paper history:

Received 11 February 2022

Received in revised form 01 May 2022

Accepted 08 May 2022

Keywords:

Hot Mix Asphalt

Reclaimed Asphalt Pavement

Rejuvenator Agents

Rutting

Finite Element Method

ABSTRACT

The rising cost of asphalt pavements reconstruction, the discussion of non-renewable resources maintenance and reducing the harmful impacts caused by reclaimed asphalt pavement (RAP) disposal have led to reusing RAP material and studying its effects on asphalt mixture performance. In this paper, recycled asphalt mixtures with higher contents of RAP were investigated, and a method was defined for evaluating the rutting behavior of conventional and recycled asphalt mixtures. Rutting is one of the major distresses in flexible pavements, commonly caused by the accumulation of permanent deformation in the asphalt layer of the pavement structure during its service life. For study purpose, conventional and recycled asphalt samples (containing 50% and 80% RAP + rejuvenator agents) were prepared. Then indirect tensile and uniaxial repeated loading tests were conducted to obtain elastic and creep properties of the studied mixtures. The available creep power-law model in ABAQUS finite element program was used to simulate rutting. After developing models, fairly acceptable outputs have been achieved regarding wheel track test results. Moreover, results showed that the addition of 50% and 80% RAP decreased rut depth by 33% and 47%, respectively.

doi: 10.5829/ije.2022.35.07a.20

1. INTRODUCTION

Over the years, pavement engineers have been developing various performance prediction methods and software programs, which some are simple and others more complex. A significant amount of effort in researches focused on predicting different distresses appearing in asphalt pavements, such as rutting, fatigue, moisture susceptibility, and thermal cracking [1-3]. The deterioration of pavements is affected by the properties of the used materials, mixing condition, pavements structure, applied traffic, and climate situation to account as the key factors [3, 4]. Models that predict different pavement deteriorations with accuracy help decision-makers for adequate and timely fund allocations for maintenance of the roads and mixture design experts to approach a better asphalt mixture that will resist longer [5-7]. Rutting is regarded as a major distress, which can even be a reason for initiating other distresses in flexible

pavements. Rutting is caused by the accumulation of permanent deformation in any of the layers in the pavement structure, which occurs due to tire pressure and axial load repetition. It typically appears as longitudinal depressions in the wheel paths, sometimes accompanied by small upheavals to the sides [8, 9]. The accumulation of permanent deformation in the asphaltic layers, mostly in warm weather conditions, is a significant component of rutting in flexible pavements. Deformation growth leads to safety performance concerns in pavements and the excessive cost of repairs [9, 10]. This is why pavement designers should keep asphalt rutting performance in mind, when designing asphalt pavements. By researching on improvements of hot-mix asphalt (HMA) materials, mix designs, and pavement assessment methods, including laboratory and field testing, an increase in pavement lifespan and considerable cost savings in pavement maintenance and rehabilitation can be achieved [11, 12].

*Corresponding Author Institutional Email: mkhabiri@yazd.ac.ir
(M. M. Khabirib)

Since hot asphalt mixtures' performance depends on factors like time, stress and temperature, it is somehow sophisticated to predict their rutting performance; therefore, it is important to utilize a suitable constitutive model when modeling the permanent deformation of asphalt mixtures. Different models such as elasticity, viscoelasticity, viscoelastoplasticity, plasticity, and creep have been used in researches to characterize asphalt behavior [13-15].

The finite element method (FEM) is now one of the most widely applied methods for solving mathematical models of many engineering problems. It is based on the idea of building a complicated object with simple blocks or dividing a complicated object into smaller and manageable pieces [16, 17]. Two types of finite element programs are available to determine the stress, strain, and deformation in flexible pavement systems, including programs developed specifically for pavement systems analysis and general-purpose finite element programs .

While EverStressFE and MICHPAVE are examples of the first type of programs, ANSYS and ABAQUS belong to the second type. The first type programs are more user-friendly and can be used by even non-professionals. However, they have some disadvantages, like MICHPAVE only gives 2D outputs. Also, both programs are designed based on local pavement specifications, making them less capable of studying varied cases. Having a strong library to simulate complex behavioral models in materials including linear, nonlinear and viscoelastic, has made ABAQUS a powerful tool allowing to consider almost all controlling parameters (cracks, damping, static or dynamic loading) has made it popular between researchers to develop 2D or 3D models because of higher accuracy than other programs and also to utilize different constitutive models and geometries in order to evaluate any structured performance [18, 19].

The construction and maintenance of pavements require large amounts of aggregates, which typically account for more than 90% of asphalt mixtures by weight [20, 21]. This is while both bitumen and aggregates used in asphalt mixtures are supplied from non-renewable resources. With the continuously increasing costs of construction materials and concern over environmental issues, the pavement industry is attracted to the use of reclaimed asphalt pavement (RAP) materials in the construction of asphalt pavement [22, 23]. Based on the mixture type, between 10 and 40% RAP materials are currently used in HMA [23, 24]. One way to promote sustainability in road construction is the feasibility of increasing RAP content in asphalt mixtures and having mixtures with similar performance characteristics as HMA. So far, different studies have been conducted on various additives, rejuvenator agents, and mixing processes to improve the rheological properties of RAP aged binder for having more recycled mixtures resistant

against common pavement distresses [25, 26]. However, many countries do not take up the opportunities because of uncertainty in performance prediction [27]. Therefore, several researchers have tried to obtain a clear and more reliable understanding of RAP asphalt mixtures' performance by using methodological and theoretical models alongside laboratory outputs [28, 29]. As mentioned earlier, rutting is one significant distress that occurs due to the repetition of external load on the pavement during its service life, so the ability to predict rutting can be used as a component in sustainable models and help increase pavements lifespan. Although, studies have shown that RAP mixtures are less vulnerable to rutting than other distress. But still, in many mechanical studies, the impact of different factors on increasing or decreasing rut depth in such mixtures is being evaluated [30-32].

In this study, two different recycled mixtures, respectively containing 50 and 80% RAP material, rejuvenated with a petroleum-based rejuvenating agent and also conventional asphalt mixture (containing 0% RAP) were assessed then an analytical method was provided to characterize the rutting behavior of studied mixtures, under the simulation of wheels repeated loading. Indirect tensile stiffness modulus (ITSM) and repeated load axial (RLA) tests were performed on the studied samples in order to assess mixtures' behavior and obtain creep power-law parameters required for modeling. Afterward, a 3D finite element model in ABAQUS software was developed. Finally, the models were evaluated and calibrated with wheel track test results .

2. MATERIALS AND SAMPLE PREPARATION

RAP materials were collected from a hot in-place asphalt rehabilitation project, which was in process on one of the highways in Guilan Province, Iran (see Figure 1). RAP asphalt binder was extracted with centrifuge extraction, using toluene as a solvent according to ASTM D2172. Both new and RAP original aggregates were siliceous type aggregates. The gradation of new (virgin) aggregates, RAP aggregates and design gradation used in



Figure 1. The RAP used in this study

this study are presented in Table 1. The design gradation is the dense gradation within upper and lower limits of the proposed gradation No. 4 of Iran Highway Asphalt Paving (IHAP) Code No.234 for surface courses (AASHTO Type IV gradation) [33]. After long-term field use, the gradation of the aged asphalt mixture usually tends to get finer. Thus, the gradation of new aggregates was set to compensate this problem in reaching the specified design gradation.

The virgin asphalt binder applied in this study was a 60/70 penetration grade base bitumen (AC 60/70) produced by Pasargad oil company. The properties of the virgin and extracted RAP asphalt binders are listed in Table 2, where the RAP binder is observed to be stiffer than the virgin binder due to aging.

Using rejuvenator agents is an effective way to restore aged binder properties. Rejuvenators are suitable for mixtures with high contents of RAP [34]. A petroleum-based rejuvenator agent with low viscosity and asphaltene contents was selected for this project. Its properties are shown in Table 3.

Three types of HMA samples were prepared in this study; accordingly, one conventional HMA mixture without RAP as a control mix and two recycled asphalt mixtures, respectively containing 50% (HMA-50%RAP) and 80% (HMA-80%RAP) RAP, were designed.

Several methods can be used to prepare recycled mixtures in laboratories, and most of them are usually

TABLE 1. Gradations (% passing) of RAP materials, new aggregates and design gradation

Sieve size (mm)	RAP	New aggregates added into		Design gradation (Target gradation for recycled mixtures)	Lower-upper limits
		recycled mixture containing 80% RAP	recycled mixture containing 50% RAP		
19	100	100	100	100	100
12.5	94	100	96.4	95.2	90-100
4.75	50	70	58	54	44-74
2.36	31	50	38.6	34.8	28-58
0.3	8	15	10.8	9.4	5-21
0.075	4	6	4.8	4.4	2-10

TABLE 2. Properties of virgin (60/70 penetration grade type) and RAP asphalt binder

Test	Virgin	RAP
Penetration (100 g, 5 s, 25°C), 0.1 mm	64	31
Ductility (25°C, 5 cm/min), cm	112	-
Softening point (°C)	51	55
Flash point (°C)	262	-

TABLE 3. Properties of the rejuvenator used in this study

Indices	Values
Viscosity (60°C, cSt)	119
Specific gravity (25 °C)	0.973
Flash point (°C)	219
TFOT aged	
Residual viscosity ratio	1.1
Mass loss percent (%)	2.7

different from what really occurs in industrial mixing methods. Here it was tried to simulate the hot in-place recycling process for producing the recycled mixtures. When producing the recycled mixtures, firstly, the rejuvenator was added into 160°C RAP and blended for 3 minutes to make the rejuvenator diffuse properly in RAP. In order to have a positive effect on the RAP binder, the optimal quantity of the rejuvenator was determined to be 7% by weight of the RAP asphalt binder. The mixing process of the computed rejuvenator agents with RAP binder is the most important part of producing recycled mixtures. Secondly, after blending the rejuvenator with RAP, the pre-prepared fresh HMA (new aggregates + virgin binder) with the right portions for each mix was added into the blend and mixed. The mixing temperature was 155°C, and the compaction temperature was 140°C for all types of mixtures. Marshall mix design according to ASTM D1559 was employed to design the mixtures. The optimum binder content was determined related to 4% air voids content in the whole mix compacted under 75 blows on each side of cylindrical samples. The optimum binder content for the conventional HMA-50%RAP and HMA-80%RAP mixtures was 5.1%, 4.8% and 4.6%, respectively.

3. LABORATORY TESTS

3. 1. Indirect Tensile Stiffness Modulus (ITSM) Test

One of the standard tests for determining the stiffness of bituminous materials is the ITSM test. In this study, the Nottingham Asphalt Tester (NAT) was used to conduct the test, which is a non-destructive method .

Asphalt mixture stiffness modulus is one of the essential mechanical properties for the analysis and design of flexible pavements. That is directly associated with the capacity of the material to distribute load [35, 36]. The stiffness of a material is also represented by the ratio between stress and strain, which is called Young's modulus of elasticity [35].

The laboratory test procedure adopted in this research was in accordance with British standard DD213. The test was held at 40°C inside the temperature-controlled cabinet, and cylindrical asphalt samples with a diameter of 101.6 mm and 63.5 ± 1.0 mm height were used.

Repeated load pulses with a given rise time of 124 ms out of a 0.1 s loading time was applied in the test. After each loading, the specimen was left to rest for 0.9 s. Based on the ITSM test, bituminous mixtures stiffness modulus can be determined using Equation (1) below:

$$S_m = \frac{L(v + 0.27)}{D \times t} \quad (1)$$

where, S_m is the stiffness modulus (MPa), L is the peak value of the applied vertical load (N), D is the mean amplitude of the horizontal deformation obtained from two or more applications of the load pulse (mm), t is the mean thickness of the test specimen (mm), and v is the Poisson's ratio (a value of 0.35 is assumed in HMA).

3.2. Repeated Load Axial (RLA) Test The RLA test can simulate actual condition better than static tests. A repeated load is a simple test for assessing the resistance to permanent deformation. The most significant result of this test is the accumulated permanent strain curve against loading cycles. Analogous to most visco-elasto-plastic materials, the creep curve of asphalt mastic can be generally divided into three stages: decelerated creep, equi-velocity creep, and accelerated creep [18, 37]. Figure 2 represents the typical three-stage permanent deformation behavior of asphalt mixture in the dynamic creep test. The strain rate shows the strain slope value in graphics to help determination of each stage. The slope of strain in the second zone is constant.

The NAT was used to conduct the test on cylindrical asphalt samples with a diameter of 101.6 mm and height of 63.5 ± 1.0 mm, following British standard DD 226: 1996. In order to determine the required parameters for finite element modeling, repeated load axial magnitude was fixed on 100 and 200 kPa at a temperature of 40°C in a temperature control cabinet. In each test, 2000 cycles were applied, including a 1.0 s loading period and a 1.0 s resting period for each cycle (4000s). Two LVDTs measured the vertical deformation of the specimens.

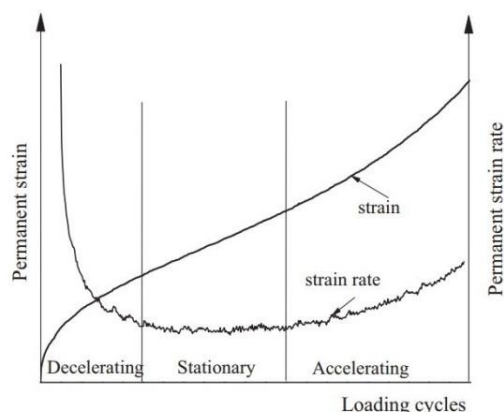


Figure 2. Typical creep curve [18]

3.3. Wheel Track Test The wheel track test is a routine test used for characterizing the rutting resistance potential of HMA mixtures in the laboratory. In wheel track test, a wheel is rolled across the surface of an asphalt sample. The wheel can also be steel or solid rubber. As the wheel tracking test is considered a simulator of in-situ pavement performance, it is a popular tool for identifying rutting potential [38, 39].

The Hamburg wheel tracking device (HWTD) was used in this study. In order to evaluate asphalt mixtures rut depth, a total wheel load of 710 N with a pace of 53 ± 2 passes per minute was applied to $30 \times 30 \times 5$ cm slab specimens with a target air void of 4%. A slab specimen under the test is shown in Figure 3. The test was conducted inside the environmental chamber at the temperature of 40°C, in which the samples were placed 4 h before testing.

4. WHEEL TRACK TEST FINITE ELEMENT MODELLING

The finite element model was developed in ABAQUS software to simulate the wheel track test and asphalt permanent deformation growth under the rolling wheel. ABAQUS is a powerful FEM program that solves different problems, using linear analyses for simple problems as well as nonlinear analyses for complicated ones [40]. Because of the large longitudinal dimension, the stress state in pavement structures can be defined as a plane stress condition. Although using a 2D model instead of a 3D model decreases the total computation time, in this study 3D models were adopted for more accuracy and better visualization. Considering the wheel track test condition, the middle section of the asphalt samples was modeled under several numbers of wheel passes to predict rut depth. The schematic diagram of the wheel track test adopted for modeling in ABAQUS is exposed in Figure 4.

Dimensions of the model were $300 \times 300 \times 50$ mm according to asphalt sample dimensions in the wheel track test. But because of the symmetry in model geometry, just half the width of the sample was modeled



Figure 3. Wheel track test

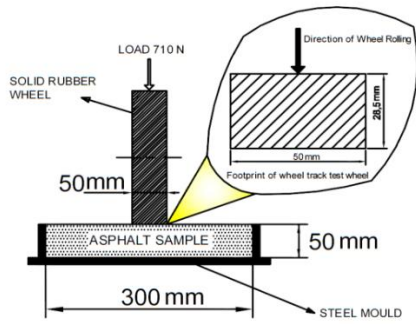


Figure 4. 2D schematic diagram of wheel track test model and wheel footprint

to show results clearly. The 3D model of the asphalt sample in ABAQUS is illustrated in Figure 5. It presented a general view of the adopted finite element meshing and boundary conditions of the model. The model consisted of 10800 elements and 12749 nodes. The vertical movements were only allowed along the edges of the model under the wheels longitudinal rolling pass, and no vertical or even horizontal movement was allowed along the other edges. A coarse or fine mesh can have negative effects on overall modeling results [41, 42]. Because of mesh size effect on models stress level the stress approach was used for mesh convergence study. Therefore the area we wanted to simulate and the stress we needed to evaluate was in the area under the wheel pass, so after several modifications and checking in mesh size we reached a constant pick stress level within the optimum size of 5*5 mm cubical elements and away from the loading area, larger elements were used that can easily be seen in Figure 5.

Considering the model requirements an 8-node Linear Brick Element (C3D8R) with the classical integration was selected in ABAQUS. The node numbering pattern is shown in Figure 6. The 8-node brick element is an equally spaced and sized element, which is one of the consistent and accurate types of elements for almost all kinds of simulations.

The footprint of the solid rubber wheel on the surface of the asphalt sample in the wheel track test is illustrated in Figure 4. The tire print can be measured using carbon paper or paint [43]. The solid rubber wheel creates

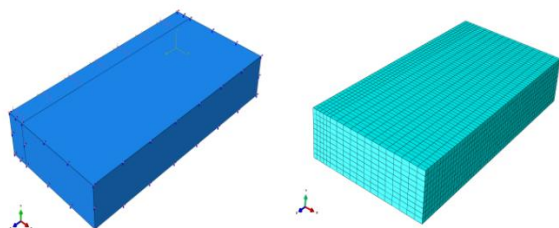


Figure 5. Asphalt sample 3D model boundary conditions and element meshes

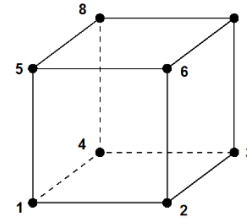


Figure 6. 8-node brick element

uniform pressures therefore the contact area between the wheel and the pavement, unlike the imprint of pneumatic tires, is exactly rectangular. The simulated footprint with the average length of 28.5 mm was used to calculate the loading time and the contact pressure. In the model, a loading pressure of 500 kPa was put along 25 mm of the middle of the sample (half the width of the wheel footprint), as presented in Figure 5.

It is somehow complex to model the wheel track test real loading mechanism with all of its details. Therefore a simple method was used to simulate the test accurately. In this modeling process, the load is instantly and statically applied to the section, and the cumulative time is considered upon the wheel passes number. This approach significantly reduces the computational time [44]. So the asphalt surface is the only node set (or true surface) in this simulation. Therefore the properties for general contact were set by ABAQUS default values [40].

The time of wheel loading in one pass is calculated according to the wheel's pace and the effective length, which the wheel and specimen are in contact [45]. Then the length of the wheel footprint is divided by the wheel speed to determine the load time. With the average wheel footprint length of 28.5 mm the loading time for each pass was calculated to be about 0.14 s. The step loading and load duration conversion described by Hua [44], as shown in Figures 7 and 8, was used in this study. In Figure 7, the movement of wheel load in the wheel track test on surface element No.1 is simulated with a step loading sequence, where the load is at its maximum from T1 to T2. While from time T0 to T1 and from time T2 to T3, the total load applied on the surface of element No.1 is not at its maximum and changes linearly from zero to

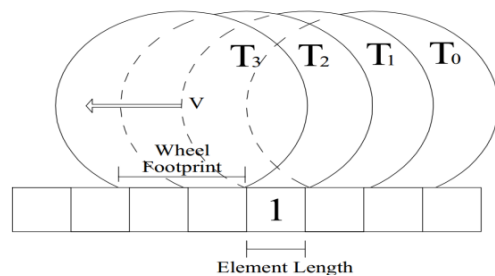


Figure 7. Wheel step by step movement and load application on element number one

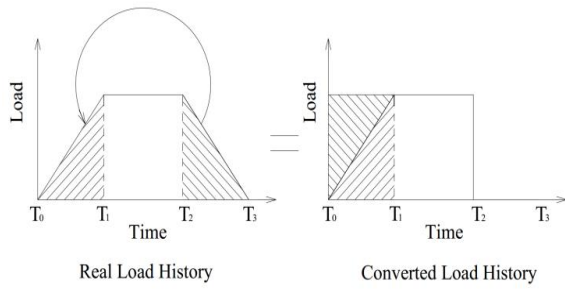


Figure 8. Load duration conversion

maximum and vice versa, respectively, which is presented in Figure 8. Based on the conversion, the T1–T2 time is 0.14 s, and the T0–T1 and T2–T3 time periods (the beginning and end length loading time) will be 0.07 s. Then, the transformed time of loading for each pass is 0.21 s; thus, the transformed time of loading for 4000 wheel pass will be 840 s.

5. CREEP POWER-LAW

Creep models can be used to characterize asphalt mixtures. The creep power-law available in the ABAQUS library is practical and suitable for problems related to the rutting of flexible pavements [11]. ABAQUS finite element program provides two versions of the creep power-law model, one time-hardening version and the other is strain-hardening version [40]. Since asphalt behavior depends on the term of time, the nonlinear time-hardening model formulated as shown in Equation (2) was utilized.

$$\dot{\epsilon} = A \sigma^n t^m \tag{2}$$

where $\dot{\epsilon}$ is the axial creep strain rate, σ is the uniaxial equivalent deviatoric stress, t is the total loading time, and A, n, m are material related parameters. Equation (3) is the integral expression of Equation (2), where ϵ is the creep strain.

$$\epsilon = \frac{A}{m+1} \sigma^n t^{m+1} \tag{3}$$

6. RESULTS AND DISCUSSION

6. 1. Indirect Tensile Stiffness Modulus (ITSM) Test Results

For both the HMA-50%RAP and HMA-80%RAP samples, stiffness modulus was higher as compared to that in conventional samples without RAP, which can be a result of RAP asphalt binder and aggregates addition. The ITSM test results for all mixtures are shown in Table 4. The obtained values are the average of three tested specimens.

6. 2. Repeated Load Axial (RLA) Test Results

The RLA test revealed the visco-elasto-plastic behavior of asphalt mixtures. According to Figure 9, test results under the axial repeated stress of 100 and 200 kPa, at temperature 40°C, show that creep curves are smooth and just have the first two stages at 100 kPa; but, at the stress of 200 kPa, the creep curve turns steeper, and the third stage of creep strain gets to start. As can be seen in Figure 9, recycled samples have lower strain values at a certain temperature and level of stress. It is generally accepted that lower strain values indicate higher rutting resistance. Samples creep rate graph is presented with CR prefix in Figure 9.

TABLE 4. ITSM values of the conventional and recycled asphalt mixtures

Mixture type	Young’s modulus of elasticity (MPa)	Poisson’s ratio
Conventional	1045	0.35
HMA-50% RAP	1447	0.35
HMA-80% RAP	1510	0.35

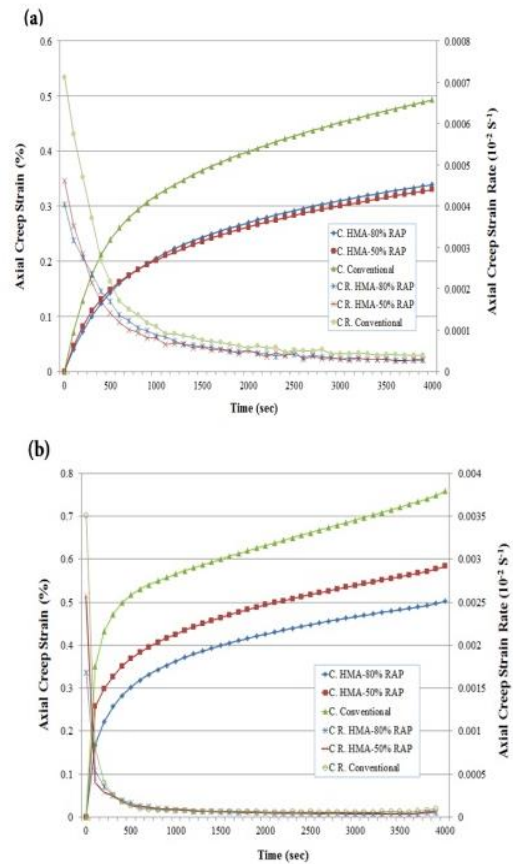


Figure 9. Creep curves and creep rate for conventional, HMA-50%RAP and HMA-80%RAP mixtures. (a) at stress of 100 kPa; (b) at stress of 200 kPa

6. 3. Wheel Track Test Results According to test results, with an increase in the number of load passes, rut depth slightly increased for all the specimens, and the HMA-80%RAP sample had the least increase in value. As presented in Table 5, the addition of RAP decreased rutting by 33 and 47% in HMA-50%RAP and the HMA-80%RAP samples, respectively, compared to the conventional sample.

6. 4. Determination of Modeling Parameters

An analysis of the visco-elasto-plastic behavior of the conventional HMA-50%RAP and HMA-80%RAP asphalt mixtures is necessary for developing the required parameters of the time-hardening version of the creep model used in ABAQUS software according to Equation 2. Equation 4 and Figure 10 show different types of strain that occur in materials with visco-elasto-plastic behavior under load applications .

$$\varepsilon(t) = \varepsilon_e + \varepsilon_p + \varepsilon_{ve}(t) + \varepsilon_{vp}(t) \tag{4}$$

where $\varepsilon(t)$ is total strain after elapses of time (t), ε_e is the elastic strain, ε_p is the plastic strain, ε_{ve} is the visco-elastic strain, ε_{vp} is the visco-plastic strain. In some other studies, thermal strain component (ε_T) is also included in total strain [46].

As presented in Figure 10, after the first loading phase, the mixture will recover some of the deflection

TABLE 5. Asphalt mixtures wheel track test results at 500 kPa stress and 40°C

Mixture type	Rut depth (mm)				
	Number of passes				
	400	1000	2000	3000	4000
Conventional	0.32	0.51	0.67	0.73	0.78
HMA-50% RAP	0.23	0.32	0.415	0.47	0.52
HMA-80% RAP	0.22	0.31	0.37	0.395	0.415

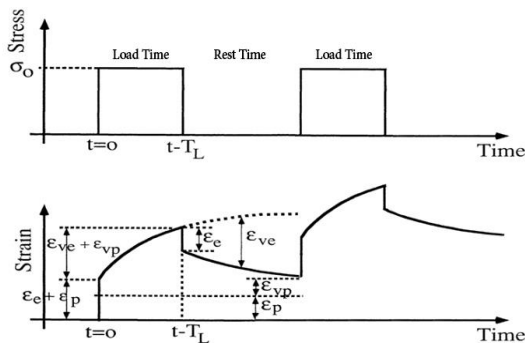


Figure 10. Asphalt stress and strain components under repeated loading

during the rest period, and the remained deflection that accumulates with each progressive loading cycle afterward makes the permanent strain. The non-recoverable strain value in asphalt is the sum of plastic and visco-plastic strain components [47].

Studies have shown that visco-plastic strain is the main contributor to permanent deformation, and at large numbers of loading cycles, plastic strain value can be considered insignificant [48, 49]. In this study, in order to model pavement behavior, the plastic strain was not separated and instead, it was considered to be a part of the visco-plastic strain; therefore, the accumulated permanent strain values obtained from RLA test were used as visco-plastic strain for determining asphalt mixtures required creep power law parameters. Besides, the permanent strain in the decelerating creep zone is mainly due to the initial air void consolidation which is not related to the asphalt mixture rutting resistance over the service life, therefore it was not considered.

The visco-plastic strain of the secondary and tertiary zones was drawn versus time for all the mixtures at the two stress levels of 100 and 200 kPa, as shown in Figure 11 on a log–log scale. The secondary zone starts from where the strain rate gets constant. The asphalt strain trend, reflected in Figure 11, shows that the samples tend to have larger strains and steeper slopes with the increase in stress level. Also, Figure 11 demonstrates that the addition of RAP in the asphalt samples can reduce strain rate.

Parameter (m) of the creep power-law model relates with parameter (β), as shown in Equation (5). According to many researches, parameter (m) has a value between -1 and 0 [50]. Average slopes of tangents in corresponding trend lines shown in Figure 11 for each mixture at 40°C, are estimated as parameter (β) value.

$$m = \beta - 1 \tag{5}$$

Parameter (β) is also used to set up a quadratic regression equation, where the $(\frac{\varepsilon_{vp}}{t^\beta})$ versus stress level relationship presented in Figure 12 for each mixture, gives a creep model as defined in Equation (6).

$$B(\sigma) = \varepsilon_{vp}(\sigma, t, N) / t^\beta \tag{6}$$

According to Figure 12, by determining the coefficients (b1 and b2), $B(\sigma)$ can be explained as a second order polynomial function presented by Equation (7). Therefore, the visco-plastic strain can be articulated as Equation (8) [50].

$$B(\sigma) = b_1\sigma + b_2\sigma^2 \tag{7}$$

$$\varepsilon_{vp}(\sigma, t, N) = (b_1\sigma + b_2\sigma^2) \times t^\beta \tag{8}$$

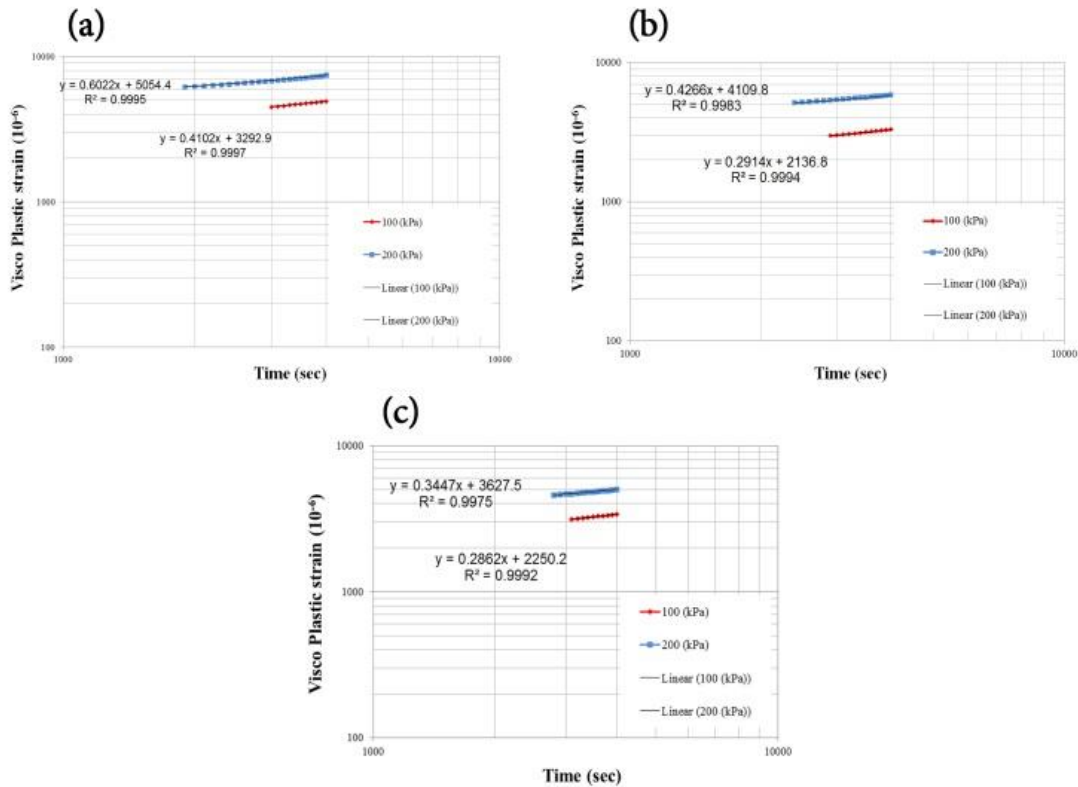


Figure 11. Visco plastic strain versus time at 40°C for (a) conventional mixtures; (b) HMA-50% RAP mixtures and (c) HMA-80% RAP mixtures

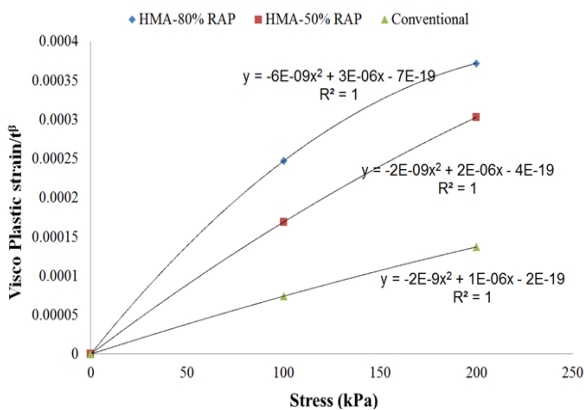


Figure 12. Visco plastic strain/ t^β versus stress relationship at 40°C for conventional mixtures; HMA-50% RAP mixtures and HMA-80% RAP mixtures

Except for parameter (m), which was directly derived from creep strain curves, other parameters of creep power-law (A) and (n) were developed by regression analysis. To do so, the solver tool in the Microsoft Excel program was used to fit Equations (3) and (8). The obtained values for creep power-law parameters are represented in Table 6. According to the parameters

TABLE 6. Asphalt mixtures creep power-law parameters

Mixture type	A ($\times 10^{-6}$)	n	m
Conventional	1.87	0.67	-0.4938
HMA-50% RAP	2.34	0.72	-0.641
HMA-80% RAP	2.65	0.72	-0.6846

determination procedure, each asphalt sample has its own set of creep parameters.

Finally, the creep law parameters and elastic properties for each mix were respectively entered in the plasticity and elasticity groups inside ABAQUS finite element program to model the asphalt wheel track test.

6. 5. Finite Element Modeling Results

ABAQUS contour plots showing the predicted deformation for all types of the studied mixtures after 4000 wheel passes at 40°C and stress level of 500 kPa are shown in Figure 13. The contour plots deformation scale factor is 30. It is shown in Figure 13 that under and near the wheels loading area, the deformation value is more than in other areas. The finite element model was also capable to predict the upward deformation of the asphalt samples, which was not managed to be recorded during the wheel

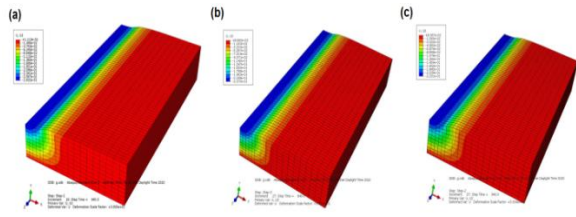


Figure 13. Predicted deformed shape of (a) conventional; (b) HMA-50% RAP and (c) HMA-80% RAP, samples after 4000 passes

track test. Maximum values of the predicted rutting for the conventional, 50 and 80% RAP asphalt samples are 0.283, 0.237 and 0.223 mm, respectively. The predicted asphalt rut depth ranking complies with the overall rank based on the wheel track test results, where HMA-80% RAP has the lowest rutting rank. One reason for the difference between the predicted and measured values is because of the mixtures mass decrease in the primary rutting stage which is not considered in the analytical creep model and the difference in asphalt samples confinement situations under the RLA compared to the wheel track test. Another probable cause for this is the axial repeated stress of 100 kPa, at temperature 40°C, having a creep rate partially interfering the second zone in studied samples, maybe not suitable enough to gain proper visco-elasto-plastic properties.

The model has the capability to be calibrated. For this purpose, some modification was applied to the initial obtained creep law parameters. The (n) parameter is stress related. As rutting evaluation in the wheel track test was executed at steady loading stress, the (n) parameter did not vary and is fixed at the original level for each sample. Parameter (A) is the value of the y-axis intercept while parameter (m) is related to the slope of the strain–time relationship curve in a log–log scale [11]. Parameters (A) and (m) were adjusted to match the rutting depth measured for the first 400 wheel passes. To reach an acceptable adjustment, new creep parameters were estimated by means of trial and error. Each time the value of (A) and (m) in the models was adjusted, and predictions were compared with measured rut depths. The adjusted parameters are presented in Table 7.

Figure 14 shows samples deformed shape by 4000 passes after calibration. Figure 15 presents the models prediction versus rutting measured at the number of

TABLE 7. Modified creep parameters values after calibration

Mixture type	A	n	m
Conventional	1.09×10^{-5}	0.67	-0.6441
HMA-50% RAP	5.68×10^{-6}	0.72	-0.6577
HMA-80% RAP	6.64×10^{-6}	0.72	-0.7515

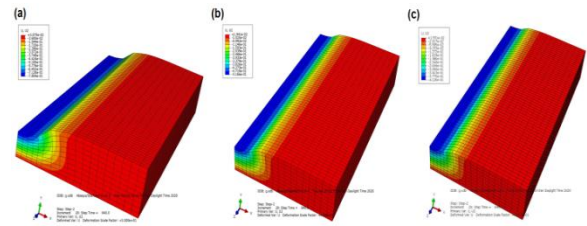


Figure 14. (a) conventional; (b) HMA-50% RAP and (c) HMA-80% RAP, samples deformation prediction shape after calibration

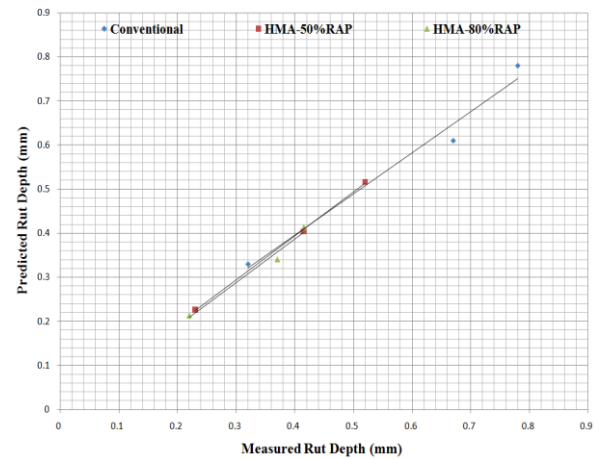


Figure 15. Relationship between Measured and Predicted rutting of asphalt samples

wheel passes 400, 2000 and 4000. As can be seen after calibrations against measured values till the first 400 passes, comparisons between the predicted rut depth in modeling and the measured rut depth in wheel track at 2000 and 4000 passes showed a difference less than 8%. It shows that the presented model can capture pavements rutting behavior for different numbers of loading cycles. Figure 15 also shows that the conventional sample had the highest rate of rutting accumulation in the early stages of loading .

7. CONCLUSIONS

In this paper, rutting performance of conventional and recycled asphalt mixtures containing high portions of RAP mixed with rejuvenator agent was investigated and simulated based on the introduced approach and laboratory performance test outputs. According to the obtained data, some conclusions are summarized as follows:

- The optimum binder content for mixes containing RAP reduced as the amount of RAP increased. The optimum binder contents were 5.1%, 4.8% and 4.6%

for conventional, 50 and 80%RAP mixtures, respectively .

- The presence of RAP in the asphalt mixtures tended to increase their stiffness and decrease their creep strain, as compared to the conventional asphalt mixtures .
- Incorporating RAP material and increasing its portion in recycled asphalt mixtures improved the rutting resistance in comparison with conventional asphalt mixture.
- RAP reduced rut depth regarding both experimental and simulation results.
- Rutting predictions of the developed finite element model were consistent with the wheel track test results.
- Regarding simulation results for both the conventional and recycled asphalt mixtures, with some tuning on the modeling parameters, the proposed method and finite element model showed to be a feasible tool for predicting asphalt mixtures rutting behavior.

It is recommended that further research can be done on profiling the RAP mixtures behavior against other prevailing distresses under different combinations of variables as a technique to produce more reliable mixtures with higher RAP percent and similar performance characteristics as HMA.

8. REFERENCES

1. Du, Y., Chen, J., Han, Z. and Liu, W., "A review on solutions for improving rutting resistance of asphalt pavement and test methods", *Construction and Building Materials*, Vol. 168, (2018), 893-905. <https://doi.org/10.1016/j.conbuildmat.2018.02.151>
2. Foroutan Mirhosseini, A., Kavussi, A., Jalal Kamali, M.H., Khabiri, M.M. and Hassani, A., "Evaluating fatigue behavior of asphalt binders and mixes containing date seed ash", *Journal of Civil Engineering and Management*, Vol. 23, No. 8, (2017), 1164-1175. <https://doi.org/10.3846/13923730.2017.1396560>
3. Han, J. and Shiwakoti, H., "Wheel tracking methods to evaluate moisture sensitivity of hot-mix asphalt mixtures", *Frontiers of Structural And Civil Engineering*, Vol. 10, No. 1, (2016), 30-43. doi: 10.1007/s11709-016-0318-1
4. Bahmani, H., Khani Sanij, H., Roshani, R., Majidi Shad, M.M., Hosseini, S.H., Edalati, M., Olazar, M. and Almasi, S., "Influence of mixing conditions of modified bitumen on the moisture sensitivity of asphalt compounds", *International Journal of Engineering*, (2022). <https://dx.doi.org/10.5829/ije.2022.35.05b.02>
5. Wang, Z., Guo, N., Wang, S. and Xu, Y., "Prediction of highway asphalt pavement performance based on markov chain and artificial neural network approach", *Journal of Supercomputing*, (2020). <https://doi.org/10.1007/s11227-020-03329-4>
6. Dave, E.V., Leon, S. and Park, K., "Thermal cracking prediction model and software for asphalt pavements", in Transportation and Development Institute Congress 2011: Integrated Transportation and Development for a Better Tomorrow., (2011), 667-676. doi: 10.1061/41167(398)64
7. Chopra, T., Parida, M., Kwatra, N. and Chopra, P., "Development of pavement distress deterioration prediction models for urban road network using genetic programming", *Advances in Civil Engineering*, Vol. 2018, (2018). <https://doi.org/10.1155/2018/1253108>
8. Khodadadi, M., Moghadas Nejad, F. and Khodaii, A., "Comparison of rut susceptibility parameters in modified bitumen with ppa", *AUT Journal of Civil Engineering*, Vol. 1, No. 2, (2017), 129-134. doi: 10.22060/ceej.2017.12383.5198
9. Xu, T. and Huang, X., "Investigation into causes of in-place rutting in asphalt pavement", *Construction and Building Materials*, Vol. 28, No. 1, (2012), 525-530. <https://doi.org/10.1016/j.conbuildmat.2011.09.007>
10. Abukhettala, M.E., "The relationship between marshall stability, flow and rutting of the new malaysian hot-mix asphalt mixtures", Universiti Teknologi Malaysia, master, (2006).
11. White, T., Haddock, J., Hand, A. and Fang, H., Contributions of pavement structural layers to rutting of hot mix asphalt pavements. Transportation research board, nchrp report 468, washington, .Dc. (2002).
12. Al-Haydari, I.S., Al-Haidari, H.S., Mohammed-Noor Khudhur, H., Waleed Jumah, N. and Abd Al-Hamza, M., "Durability and aging characteristics of sustainable paving mixture", *International Journal of Engineering, Transactions B: Applications*, Vol. 34, No. 8, (2021), 1865-1873. <https://dx.doi.org/10.5829/ije.2021.34.08b.07>
13. Behbahani, H., Ziari, H. and Kamboozia, N., "Evaluation of the visco-elasto-plastic behavior of glassphalt mixtures through generalized and classic burger's models modification", *Construction and Building Materials*, Vol. 118, (2016), 36-42. <https://doi.org/10.1016/j.conbuildmat.2016.04.157>
14. Pei, J., Fan, Z., Liu, H., Zhang, J., Li, R. and Li, Y., "Nonlinear viscoelastic model for asphalt mixture subjected to repeated loading", *Road Materials and Pavement Design*, Vol. 17, No. 4, (2016), 892-905. <https://doi.org/10.1080/14680629.2015.1137781>
15. Mirabdolazimi, S.M. and Shafabakhsh, G.A., "New model for visco-elastic behavior of asphalt mixture with combined effect of stress and temperature", *International Journal of Engineering, Transactions C: Aspects*, Vol. 31, No. 6, (2018), 894-902. <https://dx.doi.org/10.5829/ije.2018.31.06c.05>
16. Chen, X. and Liu, Y., "Finite element modeling and simulation with ansys workbench, CRC Press, (2014).
17. You, L., Yan, K. and Liu, N., "Assessing artificial neural network performance for predicting interlayer conditions and layer modulus of multi-layered flexible pavement", *Frontiers of Structural and Civil Engineering*, (2020), 1-14. <https://doi.org/10.1007/s11709-020-0609-4>
18. Zhang, J., Zhu, C., Li, X., Pei, J. and Chen, J., "Characterizing the three-stage rutting behavior of asphalt pavement with semi-rigid base by using umat in abaqus", *Construction and Building Materials*, Vol. 140, (2017), 496-507. <https://doi.org/10.1016/j.conbuildmat.2017.02.152>
19. Elseifi, M.A., Al-Qadi, I.L. and Yoo, P.J., "Viscoelastic modeling and field validation of flexible pavements", *Journal of Engineering Mechanics*, Vol. 132, No. 2, (2006), 172-178. [https://doi.org/10.1061/\(ASCE\)0733-9399\(2006\)132:2\(172\)](https://doi.org/10.1061/(ASCE)0733-9399(2006)132:2(172))
20. Huang, Y., Bird, R.N. and Heidrich, O., "A review of the use of recycled solid waste materials in asphalt pavements", *Resources, Conservation and Recycling*, Vol. 52, No. 1, (2007), 58-73. <https://doi.org/10.1016/j.resconrec.2007.02.002>
21. Khabiri, M.M., "The effect of stabilized subbase containing waste construction materials on reduction of pavement rutting depth", *Electronic Journal of Geotechnical Engineering*, Vol. 15, (2010), 1211-1219.

22. Valdés, G., Pérez-Jiménez, F., Miró, R., Martínez, A. and Botella, R., "Experimental study of recycled asphalt mixtures with high percentages of reclaimed asphalt pavement (RAP)", *Construction and Building Materials*, Vol. 25, No. 3, (2011), 1289-1297. <https://doi.org/10.1016/j.conbuildmat.2010.09.016>
23. Padula, F.R., Nicodemos, S., Mendes, J.C., Willis, R. and Taylor, A., "Evaluation of fatigue performance of high rap-wma mixtures", *International Journal of Pavement Research and Technology*, Vol. 12, No. 4, (2019), 430-434. <https://doi.org/10.1007/s42947-019-0051-y>
24. Hussain, A. and Yanjun, Q., "Effect of reclaimed asphalt pavement on the properties of asphalt binders", *Procedia Engineering*, Vol. 54, (2013), 840-850. <https://doi.org/10.1016/j.proeng.2013.03.077>
25. Pradhan, S.K. and Sahoo, U.C., "Evaluation of recycled asphalt mixtures rejuvenated with madhuca longifolia (mahua) oil", *International Journal of Pavement Research and Technology*, (2020), 1-11. <https://doi.org/10.1007/s42947-020-0279-6>
26. Saleh, M., "Laboratory evaluation of warm mix asphalt incorporating high rap proportion by using evotherm and sylvaroad additives", *Construction and Building Materials*, Vol. 114, (2016), 580-587. <https://doi.org/10.1016/j.conbuildmat.2016.03.200>
27. Thom, N. and Dawson, A., "Sustainable road design: Promoting recycling and non-conventional materials", *Sustainability*, Vol. 11, No. 21, (2019), 6106. <https://doi.org/10.3390/su11216106>
28. Zaumanis, M. and Mallick, R.B., "Finite element modeling of rejuvenator diffusion in rap binder film—simulation of plant mixing process", in Multi-scale modeling and characterization of infrastructure materials. (2013), 407-419. doi: 10.1007/978-94-007-6878-9_30
29. Yan, J., Zhu, H., Zhang, Z., Gao, L. and Charmot, S., "The theoretical analysis of the rap aged asphalt influence on the performance of asphalt emulsion cold recycled mixes", *Construction and Building Materials*, Vol. 71, (2014), 444-450. <https://doi.org/10.1016/j.conbuildmat.2014.09.002>
30. Syed, I.A., Mannan, U.A. and Tarefder, R.A., "Comparison of rut performance of asphalt concrete and binder containing warm mix additives", *International Journal of Pavement Research and Technology*, Vol. 12, No. 2, (2019), 162-169. <https://doi.org/10.1007/s42947-019-0021-4>
31. Moghadas Nejad, F., Azarhoosh, A., Hamed, G.H. and Roshani, H., "Rutting performance prediction of warm mix asphalt containing reclaimed asphalt pavements", *Road Materials and Pavement Design*, Vol. 15, No. 1, (2014), 207-219. <https://doi.org/10.1080/14680629.2013.868820>
32. Zhu, X., Sun, Y., Du, C., Wang, W., Liu, J. and Chen, J., "Rutting and fatigue performance evaluation of warm mix asphalt mastic containing high percentage of artificial rap binder", *Construction and Building Materials*, Vol. 240, (2020), 117860. <https://doi.org/10.1016/j.conbuildmat.2019.117860>
33. Code, Iran Highway Asphalt Paving. "Ministry of Road and Transportation Research and Education Center." (2003).
34. Shen, J., Amirhanian, S. and Tang, B., "Effects of rejuvenator on performance-based properties of rejuvenated asphalt binder and mixtures", *Construction and Building Materials*, Vol. 21, No. 5, (2007), 958-964. <https://doi.org/10.1016/j.conbuildmat.2006.03.006>
35. Arabani, M. and Kamboozia, N., "New achievements in visco-elastoplastic constitutive model and temperature sensitivity of glasphalt", *International Journal of Pavement Engineering*, Vol. 15, No. 9, (2014), 810-830. <https://doi.org/10.1080/10298436.2014.893317>
36. Pasetto, M. and Baldo, N., "Experimental evaluation of high performance base course and road base asphalt concrete with electric arc furnace steel slags", *Journal of Hazardous Materials*, Vol. 181, No. 1, (2010), 938-948. <https://doi.org/10.1016/j.jhazmat.2010.05.104>
37. Arabani, M. and Kamboozia, N., "The linear visco-elastic behaviour of glasphalt mixture under dynamic loading conditions", *Construction and Building Materials*, Vol. 41, (2013), 594-601. <https://doi.org/10.1016/j.conbuildmat.2012.12.023>
38. Taherkhani, H., "Experimental characterisation of the compressive permanent deformation behaviour in asphaltic mixtures", University of Nottingham, (2006).
39. Radhakrishnan, V., Chowdari, G.S., Reddy, K.S. and Chattaraj, R., "Evaluation of wheel tracking and field rutting susceptibility of dense bituminous mixes", *Road Materials and Pavement Design*, (2017), 1-20. <https://doi.org/10.1080/14680629.2017.1374998>
40. Hibbit, K., "Sorensen, Inc. (2005). ABAQUS/standard User's Manual, Version 6.5. Hibbit, Karlsson & Sorensen." Inc., Pawtucket, RI.
41. Bigdeli, M. and Monfared, V., "The prediction of stress and strain behaviors in composite gears using fem", *International Journal of Engineering, Transactions B: Applications*, Vol. 34, No. 2, (2021), 556-563. <https://dx.doi.org/10.5829/ije.2021.34.02b.29>
42. Al-Tememy, M., Al-Neami, M. and Asswad, M., "Finite element analysis on behavior of single battered pile in sandy soil under pullout loading", *International Journal of Engineering, Transactions C: Aspects*, Vol. 35, No. 06, (2022) 1127-1134. <https://dx.doi.org/10.5829/ije.2022.35.06c.04>
43. Moazami, D., Muni, R., Hamid, H. and Yusoff, Z.M., "Effect of tire footprint area in pavement response studies", *International Journal of Physical Sciences*, Vol. 6, No. 21, (2011), 5040-5047. doi: 10.5897/IJPS11.1085
44. Hua, J. "Finite element modeling and analysis of accelerated pavement testing devices and rutting phenomenon", Doctoral dissertation, Purdue University, (2000).
45. ARA, Inc., ERES Consultants Division. "Guide for Mechanistic–Empirical Design of New and Rehabilitated Pavement Structures." Final Rep., NCHRP Project 1-37A, (2004).
46. Shahbodagh, B., Habte, M., Khoshghalb, A. and Khalili, N., "A bounding surface elasto-viscoplastic constitutive model for non-isothermal cyclic analysis of asphaltic materials", *International Journal for Numerical and Analytical Methods in Geomechanics*, (2016). <https://doi.org/10.1002/nag.2574>
47. Von Quintus, H. L., "Performance prediction models in the superpave mix design system, Strategic Highway Research Program. National Research Council Washington, DC, USA, Vol. 699, (1994).
48. Uzarowski, L., "The development of asphalt mix creep parameters and finite element modeling of asphalt rutting (doctoral dissertation)", University of Waterloo, (2006).
49. Zhang, Y., Luo, R. and Lytton, R.L., "Characterizing permanent deformation and fracture of asphalt mixtures by using compressive dynamic modulus tests", *Journal of Materials in Civil Engineering*, Vol. 24, No. 7, (2011), 898-906. [https://doi.org/10.1061/\(ASCE\)MT.1943-5533.0000471](https://doi.org/10.1061/(ASCE)MT.1943-5533.0000471)
50. Perl, M., Uzan, J. and Sides, A., "Visco-elasto-plastic constitutive law for a bituminous mixture under repeated loading", *Transportation Research Record*, Vol. 911, (1983), 20-26.

Persian Abstract

چکیده

روند صعودی هزینه‌های مرمت و بازسازی خرابی‌ها در روسازی‌های آسفالتی به‌علاوه بحث حفظ منابع تجدیدناپذیر و کاهش اثرات نامطلوب زیست‌محیطی دپوی مصالح خرده آسفالتی، سازمان‌ها و نهادهای مرتبط را به استفاده از مصالح آسفالت بازیافتی در مخلوط‌های آسفالتی ترغیب نموده است. در این مطالعه نمونه‌های حاوی درصد‌های بالایی از مصالح آسفالت بازیافتی مورد بررسی قرار گرفتند و روندی برای ارزیابی رفتار شیارشدگی آسفالت‌های گرم معمول و بازیافتی ارائه گردید. شیارشدگی به عنوان یکی از خرابی‌های مطرح در روسازی‌های انعطاف‌پذیر، معمولاً به واسطه تجمع تغییر شکل ماندگار در لایه رویه آسفالتی در طول عمر خدمت‌دهی روسازی پدید می‌آید. از این رو در این مطالعه نمونه‌های معمول و بازیافتی (حاوی ۵۰ و ۸۰ درصد مصالح بازیافتی به‌علاوه مواد جوان‌کننده) تهیه گشت. سپس تست‌های مقاومت کششی غیرمستقیم و بار محوری تکرار شونده جهت بدست آوردن خصوصیات الاستیک و خزشی نمونه‌ها انجام گردید. همچنین از رابطه توانی خزش در کتابخانه نرم افزار المان محدود آباکوس برای شبیه‌سازی شیارشدگی استفاده شد. با توجه به نتایج تست ویل تراک، مدل‌های توسعه یافته شبیه‌سازی رفتار شیارشدگی توانستند خروجی‌های مناسبی ارائه نمایند. به‌علاوه نتایج آزمایشگاهی نشان داد که افزودن ۵۰٪ و ۸۰٪ خرده مصالح آسفالت بازیافتی به ترتیب سبب ۳۳٪ و ۴۷٪ کاهش در شیارشدگی نمونه‌ها گردید.
